

## Complementary Mössbauer, EPR and theoretical studies of the exchange-coupled oxoferryl porphyrin cation radical system $[(\text{Cl})\text{Fe}(\text{IV})=\text{O}(\text{TMP})\cdot]^{\dagger}$

Hauke Paulsen<sup>1</sup>, Markus Müther<sup>1</sup>, Michael Grodzicki<sup>1</sup>, Alfred X Trautwein<sup>1\*</sup>, Eckhard Bill<sup>2</sup>

<sup>1</sup> Institut für Physik, Medizinische Universität, Ratzeburger Allee 160, D-23538 Lübeck;

<sup>2</sup> Max-Planck-Institut für Strahlenchemie, Stiftstrasse 34-36, D-45470 Mülheim, Germany

(Received 19 March 1996; accepted 23 May 1996)

**Summary** — We have applied Mössbauer- and EPR spectroscopy to  $[(\text{Cl})\text{Fe}(\text{IV})=\text{O}(\text{TMP})\cdot]$  which is a synthetic analog for compound I of the heme peroxidases. The temperature- and field-dependent Mössbauer- and EPR spectra were analyzed within the spin-Hamiltonian formalism. Spectral simulations with a unique parameter set are prohibited due to the fact that several of the spin-Hamiltonian parameters cannot be determined independently and, therefore, are covariant. Theoretical considerations are discussed to reduce the allowed parameter space.

**Mössbauer spectroscopy / EPR spectroscopy / oxoferryl porphyrin radical cation system / exchange coupling**

**Résumé** — Etudes théoriques par spectroscopie Mössbauer et RPE des interactions d'échange dans le système radical cation d'une oxyferrylporphyrine. Nous avons appliqué les spectroscopies Mössbauer et RPE à l'étude de  $[(\text{Cl})\text{Fe}(\text{IV})=\text{O}(\text{TMP})\cdot]$  un analogue synthétique du composé I des peroxydases du hème. Les spectres Mössbauer et RPE en fonction de la température et du champ ont été analysés avec un formalisme d'hamiltonien de spin. Les simulations de spectres avec un ensemble unique de paramètres sont interdites en raison du fait que plusieurs paramètres de l'hamiltonien de spin ne peuvent être déterminés de manière indépendante et sont donc covariants. Des considérations théoriques sont discutées pour réduire l'espace paramétrique permis.

**spectroscopie Mössbauer / spectroscopie RPE / système radical cation d'une oxyferryl-porphyrine / interactions d'échange**

### Introduction

Investigations of the electronic structure of transition metal compounds, of the coordination geometry of the metal center, and of the nature of the metal ligand bonds have to rely on spectroscopic techniques if these compounds cannot be crystallized and X-ray structure studies cannot be performed. This is especially true for transient intermediates of catalytic reactions such as compound I of the heme peroxidases and their synthetic analogs. Mössbauer spectroscopy plays a major role in this achievement when the transition metal is  $^{57}\text{Fe}$ . This method has the advantage that all iron species in a sample are observable, irrespective of their valence or spin state. The full power of the method is obtained if, besides isomer shifts and quadrupole splittings, the magnetic hyperfine interactions are derived from temperature- and field-dependent measurements. Since the magnetic hyperfine interactions owe their origin firstly to the magnetic moments of unpaired valence electrons (spin-expectation values) and secondly to the mediation of the resulting field to the nucleus (hyperfine coupling tensor), the need arises for complemen-

tary and independent data. Electron paramagnetic resonance (EPR) is a very useful tool in this respect. As it directly detects energy splittings of the electronic spin system, the signals depend on the spin multiplicity, and on the zero-field and exchange interactions. It has been shown that the combination of Mössbauer and EPR spectroscopy provides valuable insight into the electronic structure of paramagnetic iron species [1], and also of compound I of heme peroxidases and their synthetic analogs [2–8]. The data analysis is usually based on the spin-Hamiltonian formalism. The aspect covered by the present contribution concerns problems with deriving unique spin-Hamiltonian parameters due to covariances of some of the parameters in the temperature- and field-dependent measurements. One of the key parameters for the electronic structure of oxoferryl porphyrin cation radical complexes appeared to be the exchange interaction of iron(IV) ( $S = 1$ ) and porphyrin radical ( $S' = 1/2$ ). The competition of moderately strong exchange coupling ( $J$ ) and moderately strong zero-field interaction ( $D$ ) influences spin-expectation values and effective EPR  $g$ -values significantly. Quantifications of this effect are obscured by the correlation of

<sup>†</sup> Dedicated to Prof Raymond Weiss.

\* Correspondence and reprints

local  $g$ -values and  $D$  for iron(IV), and by the unknown anisotropy contribution to the exchange interaction. Here we want to present some aspects of the theoretical and practical problems within the spin-Hamiltonian formalism in the study of the heme-peroxidase compound I analog  $[(\text{Cl})\text{Fe}(\text{IV})=\text{O}(\text{TMP})^\bullet]$ , (TMP = tetramesitylporphyrin).

### Simulation of EPR- and Mössbauer spectra within a multidimensional spin-Hamiltonian parameter space

In an  $^{57}\text{Fe}$  Mössbauer experiment the information about the electronic environment of the  $^{57}\text{Fe}$  nucleus is accessible via the hyperfine interactions between the nucleus and its surrounding electrons. The Hamiltonian which adequately describes these interactions is given by [1]:

$$H_n = \langle \vec{S} \rangle \cdot \vec{A} \cdot \vec{I} - \beta_n g_n \vec{B} \cdot \vec{I} + H_Q + \delta \quad (1)$$

The first term in (1) describes the magnetic hyperfine interaction, the second the nuclear Zeeman interaction, the third the electric quadrupole interaction and the fourth the isomer shift.  $\vec{I}$  is the nuclear spin of  $^{57}\text{Fe}$ ,  $\vec{B}$  the applied field and  $\vec{A}$  the hyperfine coupling tensor.  $\langle \vec{S} \rangle$  represents the spin-expectation values of the iron valence-electron shell.

In an oxoiron(IV) ( $S = 1$ ) porphyrin cation radical ( $S' = 1/2$ ) system the paramagnetic iron is part of an exchange-coupled pair; therefore  $\langle \vec{S} \rangle$  can only be derived from diagonalization of an electronic spin Hamiltonian which includes iron-radical spin coupling [1]:

$$H_e = D \left[ S_z^2 - \frac{1}{3} S(S+1) + \frac{E}{D} (S_x^2 - S_y^2) \right] + \beta \vec{S} \cdot \vec{g}^{\text{Fe}} \cdot \vec{B} + \beta g^{\text{radical}} \vec{S}' \cdot \vec{B} - \vec{S} \cdot \vec{J} \cdot \vec{S}' \quad (2)$$

In this expression  $\vec{S}$  and  $\vec{S}'$  are the spin operators of the ferryl iron and the cation radical, respectively.  $D$  and  $E$  are the zero-field splitting and rhombicity parameters of the ferryl iron,  $\vec{B}$  is the applied field, and  $\vec{J}$  is the spin-coupling tensor. The latter can be decomposed into an isotropic part  $\tilde{J}_0$ , and an anisotropic part  $\tilde{J}_d$ , originating from the exchange interaction and spin-dipolar interaction, respectively, between iron and the cation radical. The  $g$ -factors of the ferryl iron are related to  $D$  and  $E$  depending on orbital energy differences (vide infra), while for the  $g$ -factor of the cation radical the free-electron value  $g_e = 2.0023$  is appropriate. The various tensors ( $\vec{g}$ ,  $\vec{A}$ , electric field gradient,  $\vec{D}$ ) involved in  $H_n$  (1) and  $H_e$  (2) are assumed to be collinear, because of the stereochemistry of the system and because we found that larger rotations ( $> 10^\circ$ ) of tensor axes do not result in acceptable simulations. Even then it is by no means a simple exercise to derive a consistent set of  $H_n$ - and  $H_e$ -parameters, which allow us to simulate temperature-dependent EPR spectra and temperature- and field-dependent Mössbauer spectra, in agreement with the measured data. Since several of these parameters are strongly covariant and, hence, cannot be varied

independently, we have used experimental and theoretical criteria to classify ranges of parameter values as acceptable or as unrealistic. Taking as an example the compound I analog  $[(\text{Cl})\text{Fe}(\text{IV})=\text{O}(\text{TMP})^\bullet]$  [8], we describe in the following, step by step, how parameter values are derived and fine tuned or discarded.

### Local $g$ -factors of ferryl iron in compound I analogs

The one-electron orbital occupancy of ferryl iron in perturbed octahedral symmetry as shown in figure 1a defines as possible electronic ground state  $d_{xy}^2 d_{xz}^1 d_{yz}^1$ , which is a spin-triplet state with spin degeneracy  $2S+1$ , ( $S = 1$ ). This ground state may interact, via spin-orbit coupling, with the excited spin-triplet states, eg,  $d_{xy}^1 d_{xz}^2 d_{yz}^1$  and  $d_{xy}^1 d_{xz}^1 d_{yz}^2$ , and with spin-singlet and spin-quartet states with the result that spin degeneracy is lifted. In a perturbation treatment of the orbital-ground state  $d_{xy}^2 d_{xz}^1 d_{yz}^1$  with ligand field splitting  $\Delta_1$  (which is large in comparison to the one-electron spin-orbit coupling-constant  $\zeta$ ) the spin states are represented by their magnetic quantum numbers  $m_S = 0, \pm 1$  and their energy spacings  $D$  and  $E$  (fig 1b). Within this perturbation treatment  $D$ ,  $E$  and the  $g$ -factors of the ferryl ion are given in terms of orbital energy differences  $\Delta_1$  and  $V$ , and the spin-orbit coupling constant  $\zeta$  with the latter ranging from 350 to 400  $\text{cm}^{-1}$  for Fe(IV), depending on the amount of covalency of the 3d orbitals [9]:

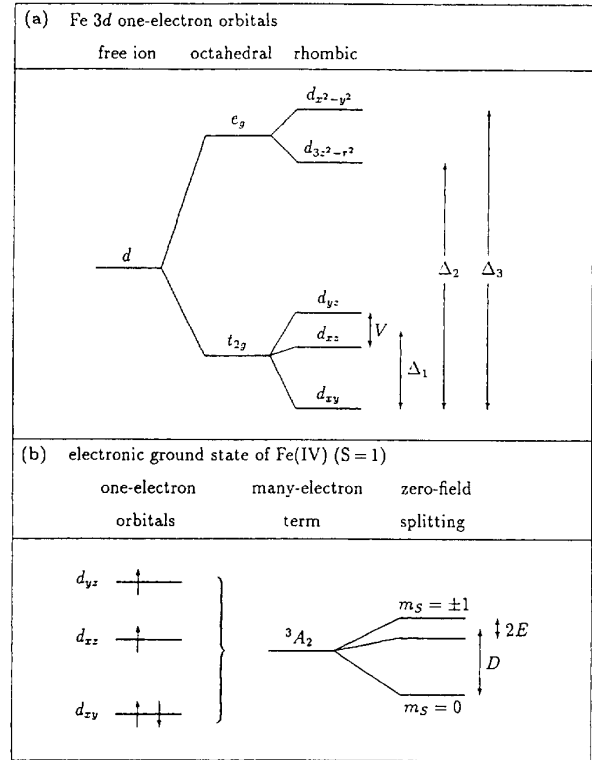
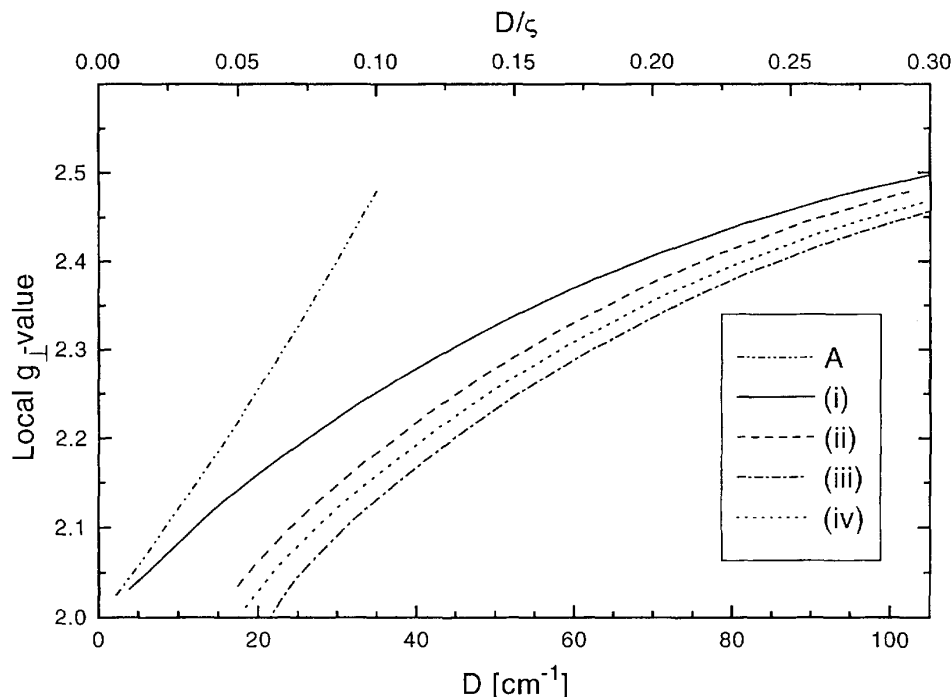


Fig 1. (a) Fe 3d one-electron orbitals and (b) electronic ground state of Fe(IV).



**Fig 2.**  $D$ -dependence of local  $g_{\perp}$ -factors of ferryl iron ( $g_{\perp} = [g_x + g_y]/2$ ), derived from the perturbation treatment of eq (3) (curve A) and from exact calculations with the following Fe  $3d$  orbital energies: (i)  $\Delta_2 = \Delta_3 = \infty$ , restricted to  $S = 1$ ; (ii)  $\Delta_2 = \Delta_3 = \infty$ , including also spin-singlet states; (iii)  $\Delta_2 = 70\zeta$ ;  $\Delta_3 = 44\zeta$ ; (iv)  $\Delta_2 = 250\zeta$ ;  $\Delta_3 = 100\zeta$ . Both (iii) and (iv) include, besides triplet-states, spin-singlet and spin-quartet states.  $\zeta$  was taken as  $350 \text{ cm}^{-1}$ .

$$\begin{aligned}
 D &= \Delta_1 \zeta^2 / (4\Delta_1^2 - V^2) \\
 E &= [(-V)/2\Delta_1]D \\
 g_x &= 2 + \left[ \zeta / \left( \Delta_1 - \frac{1}{2}V \right) \right] + \left[ \frac{1}{2} \zeta^2 / \left( \Delta_1 - \frac{1}{2}V \right)^2 \right] \\
 g_y &= 2 + \left[ \zeta / \left( \Delta_1 + \frac{1}{2}V \right) \right] + \left[ \frac{1}{2} \zeta^2 / \left( \Delta_1 + \frac{1}{2}V \right)^2 \right] \\
 g_z &= 2 - [\zeta^2 / (4\Delta_1^2 - V^2)] \quad (3)
 \end{aligned}$$

In figure 2 we compare the  $D$ -dependence ( $E = 0$ ) of  $g$ -factors as derived from the perturbation treatment of  $d_{xy}^2 d_{xz}^1 d_{yz}^1$  according to (3) with corresponding results derived from a rigorous treatment of spin-orbit coupling within the  $t_{2g}^4$  subspace restricted to  $S = 1$  states and within the complete  $(t_{2g}e_g)^4$  space including spin-singlet and spin-quartet states. The energy difference between spin-singlet and spin-quartet states is roughly approximated as  $24000 \text{ cm}^{-1}$ . For the correct interpretation of the measured effective  $g$ -factors of compound I analogs (vide infra), it is important to start with a realistic guess of local  $g$ -factors of Fe(IV); hence for  $D \sim 30 \text{ cm}^{-1}$ , for example, which is taken as upper limit, we must select from the various  $g_{\perp}$ -factors offered in figure 2. (The value for  $g_z$  will be close to 2 under this condition.) The  $g_{\perp}$ -factors derived from the perturbation calculation of  $d_{xy}^2 d_{xz}^1 d_{yz}^1$  (curve A) deviate to some extent from those derived from the exact calculation within the  $t_{2g}^4$  subspace restricted to  $S = 1$  (curve i) because for  $D > 20 \text{ cm}^{-1}$  the condition  $\zeta \ll 1\Delta_1$  is no longer valid. Both curves deviate considerably from the

$g_{\perp}$ -factors originating from the calculations in the complete  $(t_{2g}e_g)^4$  space (curves ii–iv). Among these calculations we compare the following three cases, which differ in one-electron orbital energies  $\Delta_2$  and  $\Delta_3$  of the  $e_g$  subspace: (ii)  $\Delta_2 = \Delta_3 = \infty$ , (iii)  $\Delta_2 = 70\zeta$ ;  $\Delta_3 = 44\zeta$  (taken from molecular orbital calculations), and (iv)  $\Delta_2 = 250\zeta$ ;  $\Delta_3 = 100\zeta$  ('effective' splittings regarding the large amount of covalency of the  $e_g$ -orbitals as derived from molecular orbital calculations [10]). In all cases the spin-orbit coupling-constant has been chosen as  $350 \text{ cm}^{-1}$ . Spin-polarized molecular orbital calculations have been performed for an oxoiron(IV) porphyrin system with an Fe-O bond distance of  $1.65 \text{ \AA}$  yielding strong antibonding interaction between Fe  $d_z^2$  and O  $p_z$  orbitals and an orbital ordering which corresponds to cases (iii) and (iv). This implies that  $g_{\perp}$ -factors of compound II analogs are more likely  $\sim 2.1$  and not  $\sim 2.2$  as currently used in the literature [2–7, 9].

### Effective $g$ -factors in compound I analogs

We start from oxoiron(IV), corresponding to the compound II analog, with local  $g$ -factors  $g_{\perp}^{\text{Fe}} = 2.1$ ,  $g_{\parallel}^{\text{Fe}} = 2.0$ . Provided that exchange coupling in the compound I analog between the oxoiron(IV) and the porphyrin cation radical ( $g_{x,y,z}^{\text{radical}} = 2$ ) would be strong, the  $g$ -factors corresponding to total spin ( $S = 3/2$ ) could be derived from spin-projection technique [1]:

$$g' = \frac{2}{3}g^{\text{Fe}} + \frac{1}{3}g^{\text{radical}} \quad (4a)$$

For field orientation  $\perp$  and  $\parallel$  to the molecular  $z$ -axis the result is:

$$g'_{\perp} = \frac{2}{3} \cdot 2.1 + \frac{1}{3} \cdot 2.0 = 2.067 \text{ and } g'_{\parallel} = 2.0 \quad (4b)$$

EPR spectra of the Kramers doublets of the  $S = 3/2$  multiplet are usually described by effective spin  $S^{\text{eff}} = 1/2$ . From the equivalence of matrix elements of a real operator in real spin-state space,  $\{|S, \pm 1/2\rangle\}$ , with those of an effective operator in effective spin-state space,  $\{|S^{\text{eff}} = 1/2, \pm 1/2\rangle\}$ ,

$$\langle S, m | g' \vec{B} \cdot \vec{S} | S, m' \rangle \equiv \langle \frac{1}{2}, m | g^{\text{eff}} \vec{B} \cdot \vec{S} | \frac{1}{2}, m' \rangle \quad (5)$$

the effective  $g$ -factors, as detected in the EPR experiment, are derived for arbitrary applied field  $\vec{B}$ . For the EPR-active doublet with  $m = 1/2$ ,  $m' = -1/2$ , it follows from (5):

$$\begin{aligned} \langle S, \frac{1}{2} | g'_{\perp} \vec{B} \cdot \vec{S}_+ | S, -\frac{1}{2} \rangle &= \langle \frac{1}{2}, \frac{1}{2} | g^{\text{eff}}_{\perp} \vec{B} \cdot \vec{S}_+ | \frac{1}{2}, -\frac{1}{2} \rangle \\ \vec{B} g'_{\perp} \sqrt{S(S+1)} + \frac{1}{4} &= \vec{B} g^{\text{eff}}_{\perp} \\ g'_{\perp} \left( S + \frac{1}{2} \right) &= g^{\text{eff}}_{\perp} \end{aligned} \quad (6)$$

Correspondingly, by considering  $m = m' = \pm \frac{1}{2}$ , it follows  $g^{\text{eff}}_{\parallel} = 2$ .

In summary the  $g'$ -factors of the compound I analog from above,  $g'_{\perp} = 2.067$  and  $g'_{\parallel} = 2$ , correspond to the effective values  $g^{\text{eff}}_{\perp} = 4.135$  and  $g^{\text{eff}}_{\parallel} = 2$ , provided that ferromagnetic exchange coupling between ferryl iron ( $S = 1$ ) and porphyrin cation radical ( $S' = 1/2$ ) is strong, i.e.,  $J_0 \gg D$ . In contrast to the  $g^{\text{eff}}_{\perp}$ -value of 4.135, the EPR spectrum of  $[(\text{Cl})\text{Fe}(\text{IV})=\text{O}(\text{TMP})^{\bullet}]$  (fig 3) yields the  $g^{\text{eff}}$ -values 4.230(3), 3.780(3), 1.9998(5), with the first two corresponding to the average value  $g^{\text{eff}}_{\perp} = 4.005(6)$ . The reason for this discrepancy is the fact that we are actually not concerned with an 'infinitely' strong coupled ( $J_0 \gg D$ ) iron(IV)-radical system. Instead, the exchange coupling constant  $J_0$  in  $[(\text{Cl})\text{Fe}(\text{IV})=\text{O}(\text{TMP})^{\bullet}]$  is of the order of  $D$ . This follows from a full spin-Hamiltonian analysis of the energetically lowest Kramers doublet ( $3/2, \pm 1/2$ ) for  $[(\text{Cl})\text{Fe}(\text{IV})=\text{O}(\text{TMP})^{\bullet}]$ . Taking as parameters  $S = 1$ ,  $S' = 1/2$ ,  $D = 30 \text{ cm}^{-1}$ ,  $E = 0$ ,  $B = 20 \text{ mT}$  and  $J_0 = 0.5 D, 1.0 D, 1.5 D, \dots$  we diagonalize expression (2) for each  $J_0$  value, and thus derive the energy spacing  $\Delta E$  within the EPR-active Kramers doublet. With the resonance condition

$$g^{\text{eff}}_{\perp} \beta B = \Delta E \quad (7)$$

the effective  $g_{\perp}$ -factor is derived in terms of  $J_0$ . In figure 4 we have plotted the  $g^{\text{eff}}_{\perp}$  vs  $J_0/D$  relation for two different  $D$  values (20 and  $30 \text{ cm}^{-1}$ ). This plot exhibits as important result that the ferromagnetic exchange-coupling constant  $J_0$  steeply declines when

the measured  $g^{\text{eff}}_{\perp}$ -factor takes values below 4. Figure 4 further indicates that unrealistic starting values for local  $g^{\text{Fe}}_{\perp}$ -factors considerably obscure the finding of realistic values for  $J_0$ : taking a specific value for  $D$  (eg,  $30 \text{ cm}^{-1}$ ) and then comparing solid and dashed curves, based on different estimates of  $g^{\text{Fe}}_{\perp}$ , viz, the unrealistic case (i) and the realistic case (iv) from above, respectively, reveals that the measured value  $g^{\text{eff}}_{\perp} \sim 4$  for  $[(\text{Cl})\text{Fe}(\text{IV})=\text{O}(\text{TMP})^{\bullet}]$  may yield quite different  $J_0/D$  values, namely 1.2 or 1.7 (see arrows in fig 4).

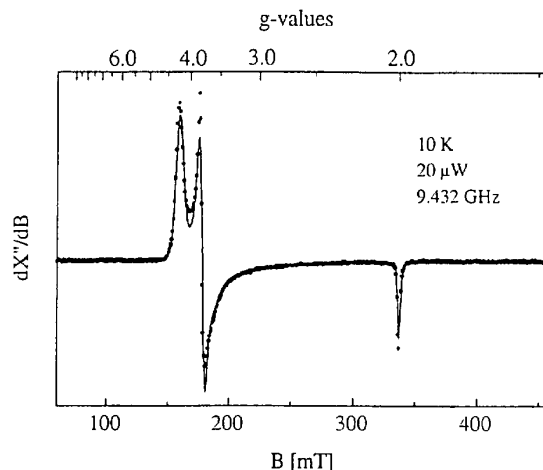


**Fig 3.** First-derivative EPR spectrum of  $[(\text{Cl})\text{Fe}(\text{IV})=\text{O}(\text{TMP})^{\bullet}]$  which was least-squares fitted with Gaussians (solid lines) of inhomogeneous line width,  $\Gamma_x = 4.8 \text{ mT}$ ,  $\Gamma_y = 7.8 \text{ mT}$ ,  $\Gamma_z = 2.8 \text{ mT}$ , yielding the  $g^{\text{eff}}$ -values 4.230(3), 3.780(3), 1.9998(5).

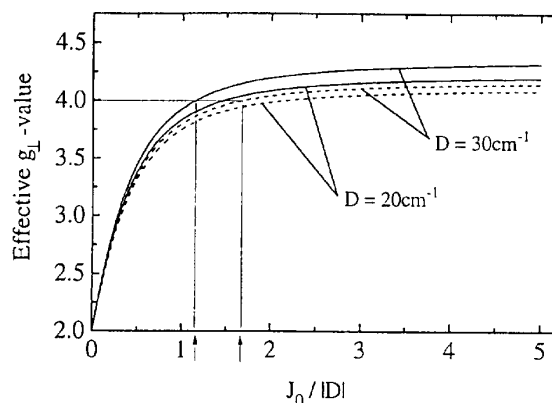


**Fig 4.** Calculated relation  $g^{\text{eff}}_{\perp}$  vs  $J_0/D$  for  $D = 30$  and  $20 \text{ cm}^{-1}$ . Starting values  $g^{\text{Fe}}_{\perp}$  are derived from a perturbation treatment (solid lines) and from the realistic case (iv) (dashed lines); see text.

### Zero-field splitting $D$

Diagonalization of the spin-Hamiltonian (2) for the simple case  $E/D = 0$  and  $B = 0$  provides the energies  $\varepsilon_{1,2}$ ,  $\varepsilon_{3,4}$  and  $\varepsilon_{4,5}$  of the three Kramers doublets,  $|3/2,$

$\pm 1/2 >$ ,  $|3/2, \pm 3/2 >$ , and  $|1/2, \pm 1/2 >$ , in analytical form as a function of  $D$  and  $J_o$ :

$$\begin{aligned}\varepsilon_{1,2} &= -\frac{1}{12}(2D - 3J_o) - \frac{1}{12}\sqrt{36D^2 + 81J_o^2 + 36DJ_o} \\ \varepsilon_{3,4} &= \frac{D}{3} - \frac{J_o}{2} \\ \varepsilon_{5,6} &= -\frac{1}{12}(2D - 3J_o) + \frac{1}{12}\sqrt{36D^2 + 81J_o^2 + 36DJ_o}\end{aligned}\quad (8)$$

Note that the local  $g$ -factors  $g_{\perp}^{\text{Fe}}$ ,  $g_{\parallel}^{\text{Fe}}$  and  $g_{x,y,z}^{\text{radical}}$  do not appear in (8) because the applied field  $\vec{B}$  is taken as zero. With  $|3/2, \pm 1/2 >$  being the EPR-active doublet it is possible to derive information about  $D$  and  $J_o$  from the temperature dependence of the doubly integrated first-derivative EPR signal intensity. Again using  $[(\text{Cl})\text{Fe(IV)}=\text{O}(\text{TMP})^\bullet]$  as an example, we have performed a least-square fit of the measured product 'intensity  $\times$  temperature' with the appropriate Boltzmann distribution:

$$I \cdot T \sim [1 + \exp(-\Delta\varepsilon'/kT) + \exp(-\Delta\varepsilon''/kT)]^{-1} \quad (9)$$

The energy differences  $\Delta\varepsilon' = \varepsilon_{3,4} - \varepsilon_{1,2}$  and  $\Delta\varepsilon'' = \varepsilon_{5,6} - \varepsilon_{1,2}$  obtained from this fit (fig 5) are  $22(3) \text{ cm}^{-1}$  and  $62(10) \text{ cm}^{-1}$  and yield with (8) the values  $D = 25(5) \text{ cm}^{-1}$  and  $J_o = 30(8) \text{ cm}^{-1}$ . We note that these values are only rough estimates because (i) the value for  $\Delta\varepsilon''$  cannot be derived more accurately by measuring temperature-dependent EPR intensities (fig 5); (ii) the rhombicity  $E$  is set equal to zero, whereas the measured difference  $\Delta g = g_y - g_x = 0.45$  (fig 3) yields according to (3) a non-zero  $E$  value; and (iii) the exchange interaction is represented by an isotropic value  $J_o$  only, however, in general anisotropy contributions  $\tilde{J}_d$  are to be expected due to spin-dipolar effects.

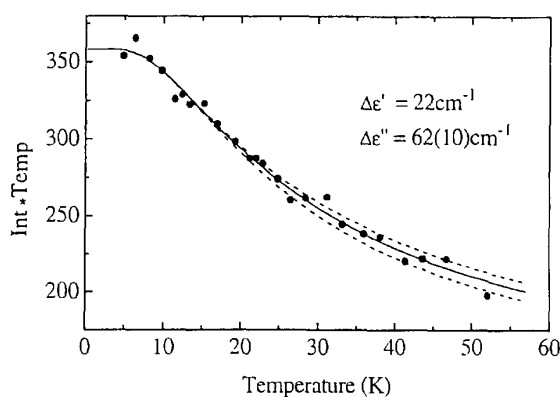


**Fig 5.** Temperature dependence of the doubly integrated first-derivative EPR signal of  $[(\text{Cl})\text{Fe(IV)}=\text{O}(\text{TMP})^\bullet]$  with a fit (solid line) of the Boltzmann population of Kramers doublets  $|3/2, \pm 1/2 >$ ,  $|3/2, \pm 3/2 >$  and  $|1/2, \pm 1/2 >$ , yielding  $\Delta\varepsilon' = 22 \text{ cm}^{-1}$  and  $\Delta\varepsilon'' = 62 \text{ cm}^{-1}$ . The dashed lines indicate the solution for  $\Delta\varepsilon'' = (62 \pm 10) \text{ cm}^{-1}$ .

Thus additional spectroscopic information is required to further adjust  $D$ ,  $E$ ,  $J_o$  and  $\tilde{J}_d$ . In principle

such information could be provided by temperature-dependent magnetic susceptibility measurements on  $[(\text{Cl})\text{Fe(IV)}=\text{O}(\text{TMP})^\bullet]$ , however, it was practically impossible to synthesize compound I analogs with 100% yield (fig 6); therefore the measured signal is obscured by the additional paramagnetism of ferric precursors and/or ferryl contaminations. Because of this preparational problem it is more suitable to apply experimental methods, such as EPR- and Mössbauer spectroscopy, which are oxidation- and spin-state specific, as well as theoretical considerations.

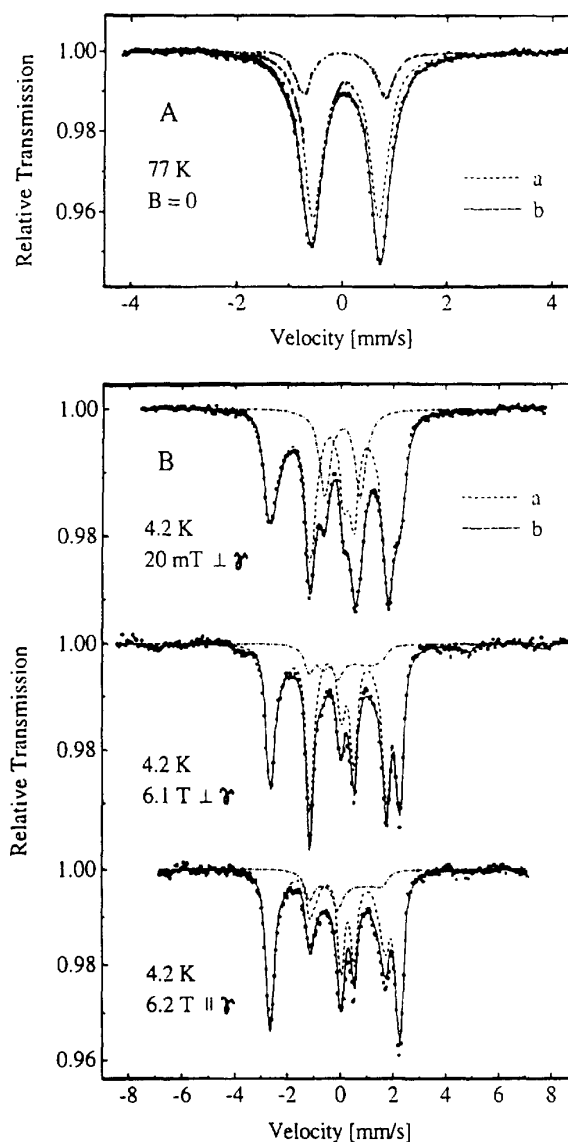


**Fig 6.** Mössbauer spectra of  $[(\text{Cl})\text{Fe(IV)}=\text{O}(\text{TMP})^\bullet]$ . (A) Measured at 77 K and  $B = 0$ ; the solid line is a least-squares fit using Lorentzians. (B) Measured at 4.2 K and applied field; the solid lines represent spin-Hamiltonian simulations using the parameter set of table I. The subspectra (a) represent the compound I analog and (b) traces of the compound II analog.

### Anisotropy contribution $J_d$

An estimate for the (spin-dipolar) anisotropy contribution, ie, the expectation value

$$\tilde{J}_d = \alpha^2 \langle \Psi | \hat{O}_{12} | \Psi \rangle \quad (10)$$

with the fine-structure constant  $\alpha \approx 1/137$  and the tensor operator

$$\hat{O}_{12} = \frac{\bar{S}_1 (3\hat{r}_{12} \cdot \hat{r}_{12}^T - 1) \bar{S}_2}{r_{12}^3} \quad (11)$$

where  $\bar{r}_{12} = \bar{r}_1 - \bar{r}_2$  and  $\hat{r} = \bar{r}/r$ , can be derived under the assumption that the interaction takes place between two magnetic orbitals,  $\psi_p(\bar{r})$  and  $\psi_o(\bar{r})$ , which are located predominantly within the porphyrin core ( $\psi_p$ ) and at the iron ( $\psi_o$ ), respectively. Both molecular orbitals (MOs) are represented as linear combination of atomic orbitals (AOs):

$$\begin{aligned} \psi_p(\bar{r}) &= \sum_m c_{dm,p} \phi_{dm}(\bar{r}) + \sum_i c_{i,p} \phi_i(\bar{r} - \bar{R}_i) \\ \psi_o(\bar{r}) &= \sum_m c_{dm,o} \phi_{dm}(\bar{r}) + \sum_i c_{i,o} \phi_i(\bar{r} - \bar{R}_i) \end{aligned} \quad (12)$$

The  $m$ -summation extends over the five  $3d$ -orbitals of iron while the second term contains the other atomic orbitals of the system. The matrix element (10) evaluated with respect to a Slater determinant built from the two MOs (12) has the following structure:

$$\tilde{J}_d = \alpha^2 \langle \psi_p(\bar{r}_1) \psi_o(\bar{r}_2) | \hat{O}_{12} | \psi_p(\bar{r}_1) \psi_o(\bar{r}_2) \rangle \quad (13)$$

An appreciable anisotropy might be expected if the integral (13) contains a sufficiently large one-center contribution due to an admixture of  $\text{Fe}(3d)$  orbitals to the magnetic porphyrin orbital, ie, if  $c_{dm,p}$  is not too small. The respective one-center integral at the iron site has the form

$$\begin{aligned} \tilde{J}_d^{(1)} &= \alpha^2 \sum_{m,m''} \sum_{m',m'''} c_{dm,p} c_{dm',o} c_{dm'',p} c_{dm''',o} \\ &\langle \phi_{dm}(\bar{r}_1) \phi_{dm'}(\bar{r}_2) | \hat{O}_{12} | \phi_{dm''}(\bar{r}_1) \phi_{dm'''}(\bar{r}_2) \rangle \end{aligned} \quad (14)$$

The evaluation of this integral is facilitated by expressing the operator  $3\hat{r} \cdot \hat{r}^T - 1$  with real spherical harmonics  $Z_{2m}(\hat{r})$  so that, eg,  $3\hat{x}^2 - 1 = \sqrt{(4\pi/5)}[\sqrt{3}Z_{22}(\hat{r}) - Z_{20}(\hat{r})]$ . In this case the components of the operator  $\hat{O}_{12}$  can be factorized by utilizing the bipolar expansion of the irregular (complex) spherical harmonics [11]:

$$\begin{aligned} &| \bar{r}_1 + \bar{r}_2 |^{-L-1} Y_{LM}(\hat{r}_1 + \hat{r}_2) \\ &= \sum_{\lambda\mu} \Gamma_{\lambda\mu}(LM) r_{<}^\lambda Y_{\lambda\mu}^*(\hat{r}_{<}) r_{>}^{-(L+\lambda+1)} Y_{\lambda+L,\mu+M}(\hat{r}_{>}) \end{aligned} \quad (15)$$

The shorthand notations  $r_{<}$  and  $r_{>}$  stand for the larger and smaller values of  $r_1$  and  $r_2$ , respectively, and

$\Gamma_{\lambda\mu}(LM)$  are expansion coefficients [11]. Retaining only the first term of this expansion with  $\lambda = \mu = 0$ , which is usually an order of magnitude larger than the higher order terms, one obtains for  $L = 2$  the simple expression

$$| \bar{r}_1 - \bar{r}_2 |^{-3} Y_{2M}(\hat{r}_1 - \hat{r}_2) = r_{>}^{-3} Y_{2M}(\hat{r}_{>}) \quad (16)$$

The matrix element (14) can thus be reduced to integrals of the type

$$\begin{aligned} &\int_0^\infty d^3r_2 \phi_{dm'}^*(\bar{r}_2) \phi_{dm'''}(\bar{r}_2) \\ &\left[ r_2^{-3} Y_{2M}(\hat{r}_2) \int_0^{r_2} \phi_{dm}^*(\bar{r}_1) \phi_{dm''}(\bar{r}_1) d^3r_1 \right. \\ &\left. + \int_{r_2}^\infty r_1^{-3} Y_{2M}(\hat{r}_1) \phi_{dm}^*(\bar{r}_1) \phi_{dm''}(\bar{r}_1) d^3r_1 \right] \end{aligned} \quad (17)$$

This expression can be further simplified on the basis of spin-polarized molecular orbital calculations for compound I analogs [10], which show that in good approximation only one  $\text{Fe}(3d)$  orbital occurs in each of the magnetic orbitals, namely  $d_{xz}$  (or  $d_{yz}$ ) in  $\psi_o(\bar{r})$  and  $d_{x^2-y^2}$  in  $\psi_p(\bar{r})$ , respectively, so that  $m = m''$  and  $m' = m'''$ . Under this condition only the term with  $M = 0$  in (16) survives, as follows from the selection rules for the Clebsch-Gordan coefficients, and therefore  $\tilde{J}_d$  is diagonal. Moreover, assuming a single-zeta radial part for the  $\text{Fe}(3d)$ -AO then

$$R_{3d}^2(r) = \frac{(2\zeta)^7}{6!} r^4 e^{-2\zeta r} \quad (18)$$

The square bracket of (17) takes the form:

$$\begin{aligned} [\dots] &= r_2^{-3} Y_{2M}(\hat{r}_2) \left\{ 1 - e^{-2\zeta r_2} \sum_6(r_2) \right\} \\ &+ \sqrt{(5/4\pi)} \frac{(2-m)}{7} \langle r^{-3} \rangle_{3d} e^{-2\zeta r_2} \sum_3(r_2) \end{aligned} \quad (19)$$

Here the abbreviation

$$\sum_n(r_2) = \sum_0^n \frac{(2\zeta r_2)^i}{i!} \quad (20)$$

has been used, and  $\langle r^{-3} \rangle_{3d}$  is the expectation value with respect to the  $\text{Fe}(3d)$ -AO. Substituting this result into (17) and performing the remaining integration over  $r_2$  yields:

$$\begin{aligned} &\langle r^{-3} \rangle_{3d} \left[ \frac{2-m'^2}{7} \left( 1 - \sum_0^6 \frac{15(3+i)!}{2^{i+1}i!6!} \right) \right. \\ &\quad \left. + \frac{2-m^2}{7} \sum_0^3 \frac{(6+i)!}{2^{i+7}i!6!} \right] \\ &= \langle r^{-3} \rangle_{3d} \frac{11}{224} (4 - m^2 - m'^2) \end{aligned} \quad (21)$$

Taking into account that  $m = 2$  and  $|m'| = 1$ , as mentioned above, the final result for the one-center contribution to the anisotropy part of the exchange coupling is obtained as

**Table I.** Parameter sets which provide successful spin-Hamiltonian simulations of Mössbauer- and EPR-spectra (fig 6b and 7).

Set	$g_{x,y,z}^{\text{radical}}$		$g_{\parallel}^{\text{Fe}}$		$g_{\perp}^{\text{Fe}}$		$g_{x,y,z}^{\text{eff}}$		$g_{\parallel}^{\text{eff}}$		Spin-Hamiltonian parameters			
	$g_{x,y,z}$	$g_{\parallel}$	$g_{\parallel}$	$g_{\parallel}$	$g_{\perp}$	$g_{\perp}$	$g_{x,y,z}$	$g_{\parallel}$	$g_{\parallel}$	$g_{\parallel}$	D (cm <sup>-1</sup> )	E/D	J <sub>0</sub> (cm <sup>-1</sup> )	J <sub>d(x,y,z)</sub> (cm <sup>-1</sup> )
I	2.003	2.016	2.110	3.780	4.230	25	0.053	42.6	1.4, 1.6, -3.0					
II	"	"	2.077	"	"	"	"	57.0	0.5, 0.5, -1.0					

Nuclear parameters (at 4.2 K)				
Set	$\delta_{\alpha-\text{Fe}}$ (mms <sup>-1</sup> )	$\Delta E_Q$ (mms <sup>-1</sup> )	$A_{\perp}/\beta_n g_n(T)$	$A_{\parallel}/\beta_n g_n(T)$
I	0.05	1.24	-25.7	-10
II	"	"	-25.0	"

$$J_{d(z)}^{(1)} = -\alpha^2 < r^{-3} >_{3d} \cdot \frac{11}{112} \cdot \sum_{m,m'} (c_{dm,p} c_{dm',o})^2 \quad (22)$$

$$J_{d(x)}^{(1)} = J_{d(y)}^{(1)} = -J_{d(z)}^{(1)}/2$$

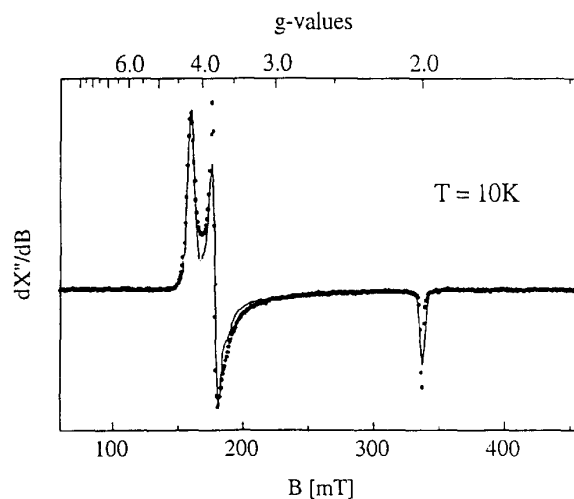
According to the results of spin-polarized molecular orbital calculations [10] representative values for the MO-coefficient  $c_{dm',o}$  are about 0.8 indicating that this MO is not a pure Fe(3d) orbital but has an appreciable amount of O(2p)-character. The Fe(3d)-coefficient  $c_{dm,p}$  of the magnetic porphyrin orbital depends strongly on the distortion of the porphyrin core and may vary between 0.1 and 0.3. With a value of 0.2 for this coefficient and of 5 au for  $< r^{-3} >_{3d}$ , a quantitative estimate for  $J_{d(z)}^{(1)}$  of  $-0.15 \text{ cm}^{-1}$  is derived. In spite of the approximations made in this calculation, namely omitting higher-order terms of the partial wave expansion in (15), and neglecting nondiagonal matrix elements of  $\tilde{J}_d$ , as well as the restriction to one-center contributions, absolute values for  $\tilde{J}_d$  larger than  $1 \text{ cm}^{-1}$  seem to be unlikely for the compound I system investigated in this work.

#### Fine-adjustment of spin-Hamiltonian parameters by simulating Mössbauer- and EPR spectra

Mössbauer measurements in zero field (fig 6a) yield isomer shift and quadrupole splitting of [(Cl)Fe(IV)=O(TMP)•] and further indicate the amount of possible preparational artefacts (ie, ferric precursors and/or ferryl contaminations) within the sample under study. Applying small or strong field, parallel or perpendicular to the  $\gamma$ -beam, provides electric and magnetic hyperfine patterns (fig 6b), which are used for the fine-adjustment of spin-Hamiltonian parameters. This procedure includes (i) deriving spin-expectation values  $\langle \tilde{S} \rangle$  from (2), for a specific experimental condition (eg, temperature and applied field) and for a given parameter set ( $D$ ,  $E/D$ ,  $S$ ,  $S'$ ,  $g_{\parallel}^{\text{Fe}}$ ,  $g_{\perp}^{\text{Fe}}$ ,  $g_{x,y,z}^{\text{radical}}$ ,  $J_0$ ,  $J_{d(x,y,z)}$ ); (ii) using  $\langle \tilde{S} \rangle$  in (1) and simulating the Mössbauer spectrum for this experimental condition; and (iii) varying  $D$ ,  $E/D$ ,  $J_0$  and  $J_d$  until the simulated and measured spectra coincide.

The simulations of measured Mössbauer spectra (solid lines in figure 6b) and of the measured EPR spectrum (fig 7) of [(Cl)Fe(IV)=O(TMP)•] are achieved

within a parameter space as indicated by the two sets I and II of values in table I and by the covariance of  $g_{\perp}^{\text{Fe}}$  and  $J_{d(z)}$  in figure 8. According to our theoretical estimates from above, ie,  $g_{\perp}^{\text{Fe}} < 2.1$  and  $|J_{d(z)}| < 1 \text{ cm}^{-1}$ , we consider the values summarized in II (table I) as the parameter set, which provides a consistent view of the various electronic and magnetic interactions in the spin-Hamiltonian (2) of the compound I analog [(Cl)Fe(IV)=O(TMP)•]. The agreement between the simulated and measured Mössbauer spectra is nearly perfect (fig 6b) while slight deviations remain between the simulated and measured EPR spectrum (in the 200 mT region, fig 7). Further fine-adjustment of parameters in order to remove this minor deviation does not provide a gain in information because of the evident covariance of parameters.

**Fig 7.** First-derivative EPR spectrum of [(Cl)Fe(IV)=O(TMP)•] simulated with the parameter set of table I.

#### Conclusion

From the spin-Hamiltonian analysis of measured Mössbauer- and EPR spectra of the compound I analog [(Cl)Fe(IV)=O(TMP)•] we conclude that successful spectral simulations are not possible with a unique parameter set. Instead, a whole parameter space is available due to the fact that several of the parameters are

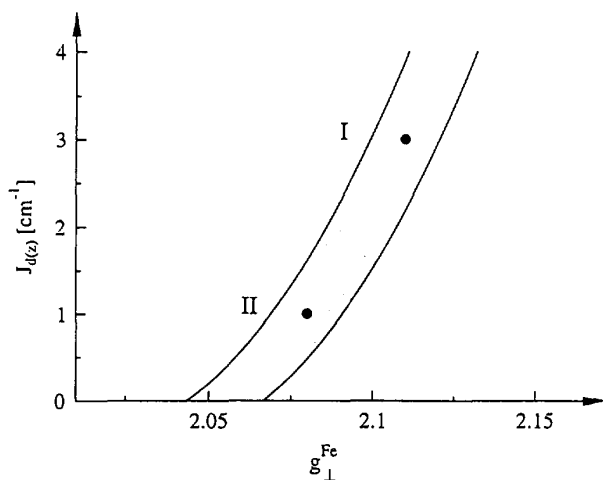


Fig 8. Covariance of  $g_{\perp}^{\text{Fe}}$  and  $J_{d(z)}$ . The area between the two solid lines defines the parameter space within which the spectra in figure 6b and figure 7 can be simulated. I and II corresponds to the two parameter sets summarized in table I.

covariant (ie,  $g_{\perp}^{\text{Fe}}$ ,  $D$ ,  $J_0$ ,  $J_{d(z)}$ ), because they cannot be determined independently. Therefore theoretical considerations are also used to provide realistic estimates of  $g_{\perp}^{\text{Fe}}$ ,  $D$  and  $J_{d(z)}$  and thus to reduce the allowed parameter space.

When comparing various compound I systems, either enzymes or their synthetic analogs, it is more important to derive trends than to obtain correct absolute values. We therefore suggest using strictly the same  $J_{d(z)}$ -value for all systems under study; only if this first attempt to simulate measured Mössbauer- and EPR spectra fails, should variations of  $J_{d(z)}$  be considered. This was also the procedure for deriving trends of the isotropic exchange interaction  $J_0$  between ferryl iron ( $S = 1$ ) and porphyrin radical ( $S' = 1/2$ ) when varying the coordination geometry of synthetic compound I analogs [6, 12].

## Acknowledgments

This work is part of a long and successful collaborations with the group of Raymond Weiss (Strasbourg, France) and Avram Gold (Chapel Hill, USA), which we gratefully acknowledge. We also acknowledge the financial support by the Deutsche Forschungsgemeinschaft, by the Alexander von Humboldt foundation and by a European Union Human Capital and Mobility grant to the MASIMO network (ERBCHRX-CT-920072).

## References

- 1 Trautwein AX, Bill E, Bominaar EL, Winkler H, *Structure and Bonding* (1991) 78, 1-95
- 2 Schulz CE, Rutter R, Sage JT, Debrunner PG, Hager LP, *Biochemistry* (1984) 23, 4743-4754
- 3 Rutter R, Hager LP, Dhonau H, Hendrich M, Valentine M, Debrunner PG, *Biochemistry* (1984) 23, 6809-6816
- 4 Boso B, Lang G, McMurry TJ, Groves JT, *J Chem Phys* (1983) 79, 1122-1126
- 5 Bill E, Ding XQ, Bominaar EL, Trautwein AX, Winkler H, Mandon D, Weiss R, Gold A, Jayaraj K, Hatfield WE, Kirk ML, *Eur J Biochem* (1990) 188, 665-672
- 6 Mandon D, Weiss R, Jayaraj K, Gold A, Terner J, Bill E, Trautwein AX, *Inorg Chem* (1992) 31, 4404-4409
- 7 Jayaraj K, Gold A, Austin RN, Mandon D, Weiss R, Terner J, Bill E, Mütter M, Trautwein AX, *J Am Chem Soc* (1995) 117, 9079-9080
- 8 Mütter M, PhD-thesis, Medizinische Universität Lübeck, Germany, 1996
- 9 Oosterhuis WT, Lang G, *J Chem Phys* (1973) 58, 4757-4765
- 10 Antony J, Grodzicki M, Trautwein AX, to be published
- 11 Steinborn EO, Ruedenberg K, *Adv Quant Chem* (1973) 7, 1-81
- 12 Mandon D, habilitations thesis, Université Louis-Pasteur, Strasbourg, France, 1995